



Heriot-Watt University  
Research Gateway

## Substantial carbon drawdown potential from enhanced rock weathering in the United Kingdom

### Citation for published version:

Kantzas, EP, Val Martin, M, Lomas, MR, Eufrazio, RM, Renforth, P, Lewis, AL, Taylor, LL, Mecure, J-F, Pollitt, H, Vercoulen, PV, Vakilifard, N, Holden, PB, Edwards, NR, Koh, L, Pidgeon, NF, Banwart, SA & Beerling, DJ 2022, 'Substantial carbon drawdown potential from enhanced rock weathering in the United Kingdom', *Nature Geoscience*, vol. 15, no. 5, pp. 382–389. <https://doi.org/10.1038/s41561-022-00925-2>

### Digital Object Identifier (DOI):

[10.1038/s41561-022-00925-2](https://doi.org/10.1038/s41561-022-00925-2)

### Link:

[Link to publication record in Heriot-Watt Research Portal](#)

### Document Version:

Peer reviewed version

### Published In:

Nature Geoscience

### Publisher Rights Statement:

The version of record of this article, first published in Nature Geoscience, is available online at Publisher's website: <http://dx.doi.org/10.1038/s41561-022-00925-2>

### General rights

Copyright for the publications made accessible via Heriot-Watt Research Portal is retained by the author(s) and / or other copyright owners and it is a condition of accessing these publications that users recognise and abide by the legal requirements associated with these rights.

### Take down policy

Heriot-Watt University has made every reasonable effort to ensure that the content in Heriot-Watt Research Portal complies with UK legislation. If you believe that the public display of this file breaches copyright please contact [open.access@hw.ac.uk](mailto:open.access@hw.ac.uk) providing details, and we will remove access to the work immediately and investigate your claim.

# Substantial carbon drawdown potential from enhanced rock weathering in the UK

Euripides Kantzas<sup>1</sup>, Maria Val Martin<sup>1</sup>, Mark R. Lomas<sup>1</sup>, Rafael M. Eufrazio<sup>2</sup>, Phil Renforth<sup>3</sup>, Amy L. Lewis<sup>1</sup>, Lyla L. Taylor<sup>1</sup>, Jean-Francois Mecure<sup>4,5</sup>, Hector Pollitt<sup>5,6</sup>, Pim V. Vercoulen<sup>5,6</sup>, Negar Vakilifard<sup>7</sup>, Philip B. Holden<sup>7</sup>, Neil R. Edwards<sup>5,7</sup>, Lenny Koh<sup>2</sup>, Nick F. Pidgeon<sup>8</sup>, Steven A. Banwart<sup>9,10</sup> and David J. Beerling<sup>1\*</sup>

<sup>1</sup>Leverhulme Centre for Climate Change Mitigation, School of Biosciences, University of Sheffield, Sheffield S10 2TN, UK

<sup>2</sup>Advanced Resource Efficiency Centre, Management School, University of Sheffield, Sheffield S10 1FL, UK

<sup>3</sup>School of Engineering and Physical Sciences, Heriot-Watt University, Edinburgh Campus, Edinburgh EH14 4AS, UK

<sup>4</sup>Global Systems Institute, Department of Geography, University of Exeter, Exeter, UK

<sup>5</sup>Cambridge Centre for Energy, Environment and Natural Resource Governance, University of Cambridge, Cambridge, CB3 9EP, UK

<sup>6</sup>Cambridge Econometrics Ltd, Covent Garden, Cambridge CB1 2HT, UK

<sup>7</sup>Environment, Earth and Ecosystems, The Open University, Milton Keynes, MK7 6AA, UK

<sup>8</sup>Understanding Risk Research Group, School of Psychology, Cardiff University, Cardiff CF10 3AT, UK

<sup>9</sup>Global Food and Environment Institute, University of Leeds, Leeds LS2 9JT, UK

<sup>10</sup>School of Earth and Environment, University of Leeds, Leeds LS2 9JT, UK

\*e-mail: [d.j.beerling@sheffield.ac.uk](mailto:d.j.beerling@sheffield.ac.uk)

**Achieving national targets for net-zero carbon emissions will require strategies compatible with rising agricultural production. One possible method for removing atmospheric carbon dioxide is enhanced rock weathering by modifying soils with crushed silicate rocks, such as basalt. Here, we use dynamic carbon budget modelling to assess the potential benefits of implementing enhanced rock weathering strategies across UK arable croplands. We find that enhanced rock weathering could deliver a net carbon dioxide removal of 6-30 Mt CO<sub>2</sub> yr<sup>-1</sup> for the UK by 2050, representing up to 45% of the atmospheric carbon removal required nationally to meet net-zero. This suggests enhanced rock weathering could play a crucial role in national climate mitigation strategies if it were to gain acceptance across national political, local community and farm scales. We show that it is feasible to eliminate the energy-demanding requirement for milling rocks to fine particle sizes. Co-benefits of enhanced rock weathering include substantial mitigation of nitrous oxide, the third most important greenhouse gas, widespread reversal of soil acidification, and considerable cost savings from reduced fertilizer usage. Our analyses provide a guide for other nations to pursue carbon dioxide removal ambitions and decarbonise agriculture, a key source of greenhouse gases.**

Governments worldwide are increasingly translating the UNFCC Paris Agreement into national strategies for achieving net-zero carbon emissions by 2050. More than 120 nations have set full decarbonization goals that account for 51% of global CO<sub>2</sub> emissions, with the UK amongst several of these nations legislating for net-zero<sup>1</sup>. The UK, where the industrial revolution driven by burning fossil fuels originated, is responsible for ~ 5% of cumulative CO<sub>2</sub> emissions 1751-2018 that drive climate change<sup>2</sup>. Carbon emissions in the UK have declined by 43 percent between 1990 and 2018 due to the rise of renewables, and the transition from coal to natural gas, while growing the economy by 75%<sup>3</sup>. Continued phase out of emissions is, however, required to meet the UK's net-zero commitment together with the capture and storage of residual emissions using Carbon Dioxide Removal (CDR) technologies and a strengthening of nature-based carbon sinks<sup>4</sup>.

Enhanced rock weathering (ERW), a CDR strategy based on amending soils with crushed calcium- and magnesium-rich silicate rocks, aims to accelerate natural CO<sub>2</sub> sequestration processes<sup>5-8</sup>. Global potential for ERW deployed on croplands to draw down CO<sub>2</sub> is substantial, estimated at up to net 2 Gt CO<sub>2</sub> per year<sup>6</sup>, with co-benefits for production<sup>9-11</sup>, soil restoration and ocean acidification<sup>7,8,12</sup>. Agricultural co-benefits can create demand for ERW deployment which is unaffected by a diminishing income from carbon-tax receipts generated by other CDR technologies as the transition to clean energy advances and emissions approach net-zero<sup>13</sup>. Global action on CDR, and hence progress to net-zero, requires leadership from early-adopting countries through their

development of flexible action plans to support policymakers of other nations. Assessment of the contribution of ERW to the UK's net-zero commitment is therefore required, given it is a CDR strategy for assisting with complete decarbonization whilst improving food production and rebuilding soils degraded by intensified land management<sup>9</sup>.

Here we examine in detail the technical potential of ERW implementation on arable croplands in a national net-zero context and provide a blueprint by which nations may proceed with this CDR technology as part of their legislated plans for decarbonisation. Using coupled climate-carbon-nitrogen cycle modelling of ERW (Methods and Extended Data Fig. 1), we constructed dynamic UK net 2020-2070 carbon removal budgets and CDR costs after accounting for secondary CO<sub>2</sub> emissions from the ERW supply chain (Methods and Extended Data Fig. 2). Coupled carbon and nitrogen cycle ERW modelling provides the fundamental advance for assessing the effects of cropland nitrogen fertilizers on the soil alkalinity balance and mineral weathering kinetics (Methods and Extended Data Fig. 3; Supplementary Information), and ERW-related mitigation of nitrous oxide (N<sub>2</sub>O) emissions from agricultural soils<sup>14</sup>. Nitrous oxide is a key long-lived greenhouse gas and important stratospheric ozone depleting substance<sup>15</sup>; UK agriculture accounts for 75% of N<sub>2</sub>O emissions nationally with high external costs (~£1 billion per year)<sup>16</sup>. Our analysis, constrained by future energy policies<sup>17</sup>, utilizes basalt as an abundant natural silicate rock suitable for ERW with croplands<sup>9,10,11</sup>, with low- (S1), medium- (S2), and high- (S3) extraction scenarios between 2035-2050 (Methods and Extended Data Fig. 4; Supplementary Information).

### **Patterns of cropland CDR**

Across low-, medium- and high-resource basalt supply scenarios (S1 to S3), ERW implementation on arable lands is simulated to remove 6-30 Mt CO<sub>2</sub> yr<sup>-1</sup> by 2050 (**Fig. 1, a-c**), i.e. up to 45% of the CO<sub>2</sub> emissions removal required for UK net-zero (balanced net-zero pathway engineered carbon removal requirement ~58 Mt CO<sub>2</sub> yr<sup>-1</sup>; range 45-112 Mt CO<sub>2</sub> yr<sup>-1</sup>)<sup>4</sup>. Modelled maximum CDR rates are predominantly governed by geographical extent of ERW application that increases as resource provision allows (**Fig. 1 a-c**). Year-on-year legacy effects are also important. CDR rates per unit area increase over time with successive annual applications of rock dust, even after land area of deployment remains constant. These effects are evident in all scenarios when basalt extraction levels off and result from slower weathering silicate minerals continuing to capture CO<sub>2</sub> in years post-application, before they are fully dissolved<sup>6</sup>. By quantifying geochemical dissolution rates

governing ERW and legacy effects, our simulations indicate the CDR potential of ERW rise over time to become over double that suggested by prior mass balance estimates<sup>18-20</sup>.

Net-zero pathways for greenhouse gas removal internationally<sup>21</sup>, and in the UK<sup>4</sup>, have tended to focus narrowly on Bioenergy with Carbon Capture and Storage (BECCS), and Direct Air Carbon Capture and Storage (DACCS). However, our new results indicate ERW can be an important overlooked component of national CDR technology net-zero portfolios working synergistically with croplands rather than competing with them as large-scale deployment of BECCS might. In S1, for example, ERW reaches a net CDR of 5 Mt CO<sub>2</sub> yr<sup>-1</sup> by 2050, equalling the DACCS estimate<sup>5</sup>, and closer to 10 Mt CO<sub>2</sub> yr<sup>-1</sup> by 2060 (**Fig. 1a**). In the highest resource scenario, S3, ERW delivers approximately half of the net CDR forecast for UK BECCS facilities<sup>5</sup> by 2050 (**Fig. 1c**).

Milling rocks to fine particle sizes is the most energy demanding step in the ERW supply chain<sup>18,22</sup>. We therefore assess a range of options for milled rock particle sizes, as defined by *p*80 (i.e., 80% of the particles having diameter of less than or equal to the specified value), and associated energy demands across scenarios S1 to S3 (**Fig. 1 d-f**). For all scenarios, we show particle size typically has a rather small effect on net CDR for the first 10-20 years of implementation, as indicated by flat CDR isolines. In the model, ERW deployment locations are prioritised over time, starting from high and progressing to low weathering potential. Prioritization of sites with high weathering potential in the first couple of decades means basalt particles are weathered rapidly regardless of size, a result verified with soil column experiments<sup>23</sup>. In S2, for example, a drawdown of 3 Mt CO<sub>2</sub> yr<sup>-1</sup> in 2035 with a *p*80 particle size of 500 μm, is achieved only 5 years earlier by milling to a *p*80 of 10 μm. Our dynamic simulations of temporal ERW carbon budgets, together with recent experimental findings<sup>23</sup>, challenge the assumption that rocks must be ground finely to accelerate dissolution for effective CDR<sup>7,8,18,22</sup>. Coarser particles minimise health and safety risks when handling rock dust, in addition to reducing energy demand. However, as S2 and S3 encompass rock dust application on more agricultural land post-2040, with a greater proportion of sub-optimal weathering locations, the dissolution of small particles becomes relevant and the effect of *p*80 on net CDR increasingly apparent.

Energy requirements for delivering ERW are generally low. Pre-2035, the energy demand for rock grinding is minimal across all three scenarios ~1 TWh yr<sup>-1</sup>; less than 0.2% of the UK's power production (Extended Data Fig. 5). Post-2040, the energy demand for grinding an increase rock mass to be distributed across an expanding area of arable land increases. However, limiting grinding to achieve rock dust with a *p*80 of 100 μm or more, keeps energy demand to less than or equal to 4

TWh yr<sup>-1</sup>, or 0.6% of UK production for all scenarios. These results mitigate prior concerns that undertaking extensive deployment of ERW in the UK may compromise energy security<sup>13</sup>.

Reducing cumulative CO<sub>2</sub> emissions on the pathway to net-zero helps minimise the UK's contribution to the remaining future carbon budget consistent with keeping warming below a given level<sup>24</sup>. Assuming ERW practices are maintained between 2020 and 2070, the resulting cumulative net CO<sub>2</sub> drawdown is simulated to be 200, 410, and 800 Mt CO<sub>2</sub> by 2070 (**Fig. 1 g-i**). Longer-term compensatory ocean outgassing and sediment CaCO<sub>3</sub> uptake could reduce net CDR effectiveness by 10-15% by 2070 (Extended Data Fig. 6). Attained over 50 years with ERW, these cumulative CDR ranges compare with an estimated ~696 Mt CO<sub>2</sub> sequestration over 100 years for afforestation in organic soils of the Scottish uplands<sup>24</sup> and avoid possible soil carbon loss from tree planting<sup>25</sup> and sustained long-term management requirements. More broadly, cumulative ERW-based CDR ranges are comparable to CO<sub>2</sub> removal estimates for UK woodland creation schemes aligned to a balanced net-zero framework (112 Mt CO<sub>2</sub> by 2050 and ~300 Mt CO<sub>2</sub> by 2070)<sup>26</sup>. Breakdown of cumulative CDR by region reveals marked shifts in regional contributions from S1 to S3, with increasing contribution over time of croplands in Scotland, north-eastern and southwest England, and the midlands. These regions have acidic soils where early deployment offers increasing CDR over time from legacy weathering effects. The more aggressive CDR strategy of S3 requires less optimal regions for ERW with the lowest rainfall (southeast and eastern England).

Mapped UK-wide CDR rates per unit area provide fine-scale estimates of modelled carbon removal potential across space and time provide an important tool for precisely targeting ERW interventions (**Fig. 2, a-c**). Results highlight the limited cropland area required for CDR by ERW in the first couple of decades in scenarios 1 and 2, and the rise in CDR per unit area over time. Across all decades and scenarios our geospatial net CDR estimates typically exceed low-carbon farming practices forming part of net zero pathways for agriculture<sup>4</sup>, including switching to less intensive tillage (typically ~1 t CO<sub>2</sub> ha<sup>-1</sup> yr<sup>-1</sup>)<sup>27</sup>, conversion of arable land to ley pasture (~1 to 5 t CO<sub>2</sub> ha<sup>-1</sup> yr<sup>-1</sup>)<sup>28</sup>, and inclusion of cover crops in cropping systems (1.1 ± 0.3 t CO<sub>2</sub> ha<sup>-1</sup> yr<sup>-1</sup>)<sup>29</sup>.

Underlying the geospatial maps of net CDR are strong cycles in alkalinity generation and soil pH, and intra-annual dissolution/precipitation of soil carbonates, driven by seasonal climate and crop production effects (Extended Data Fig. 7). These results show a decline in the periodic dissolution of soil (pedogenic) carbonates over decades as the cumulative effect of alkalinity systematically raises the seasonal minimum in soil pH and drives a steady increase in the net CDR per unit area each year. Rising alkalinity over time increases the soil buffer capacity, which reduces

the risk of pH reversal, thereby improving security of CO<sub>2</sub> storage. These results for the UK maritime climate, consistent with soil carbonate accumulation and persistent in arid systems<sup>30</sup>, raise the monitoring, verification and reporting challenge of quantifying seasonal dynamics of soil carbonates, and soil fluid alkalinity discharge, over multiple field seasons.

### Costs of cropland CDR

Costs of CDR are required to evaluate commercial feasibility, permit comparison with other CDR technologies, and for governments to understand the carbon price required to pay for it. Between 2020-2070, CDR costs fall from £200-250 t<sup>-1</sup> CO<sub>2</sub> yr<sup>-1</sup> in 2020 to £80-110 t<sup>-1</sup> CO<sub>2</sub> by 2070 (**Fig. 2 a-c**). Modelled longer-term cost trends are driven by rising CDR with successive rock dust applications (**Fig. 1 a-c**) and declining renewable energy prices (Methods and Extended Data Fig. 8). Grinding rocks to smaller particle sizes carries a minor financial penalty. As geographical deployment of ERW increases in S3, the price of CDR rises transiently 2030-2050 due to higher total energy costs associated with grinding more rock, and the requirement for more extensive logistical operations, particularly spreading of the rock dust over farms. However, it subsequently falls as CDR rates increase with repeated rock dust applications (**Fig. 1**). The dominant cost elements are electricity for rock grinding and fuel for spreading the milled rock on farmland (**Fig. 3d-f**). Mineral P- and K- nutrient fertilizers are expensive (£300-400 and £250-300 t<sup>-1</sup> for P and K fertilizers, respectively)<sup>31</sup> and fertilizer application rates per unit land area typical for arable crops (Extended Data Fig. 9) give savings sufficient to cover transport costs (**Fig. 3 d-f**).

Modelled average CDR costs for ERW practices are towards the lower-end of the range for BECCS, which varies widely across sectors<sup>4</sup> (£70-275 t<sup>-1</sup> CO<sub>2</sub>), and half that estimated for early-stage DACCS plants. DACCS CDR has an indicative price of £400 t<sup>-1</sup> CO<sub>2</sub> during the 2020s and £180 t<sup>-1</sup> CO<sub>2</sub> by 2050 as the technology develops and scales up globally<sup>4,21</sup>. ERW is thus competitive relative to these industrial CDR technologies that will also be required to help achieve net-zero emissions.

Fine-scale spatial and temporal assessment of CDR costs (**Fig. 4, a-c**), combined with analysis of regional CO<sub>2</sub> drawdown (**Fig. 2, a-c**), informs geographical prioritisation of near-term opportunities for rapid ERW deployment and public consultations on these activities. Costs in all scenarios decrease through time as CDR rises, with geographical variations in CDR costs approximately 2-fold by 2050-2060. These patterns reflect differences in CDR and, to a lesser extent, transport distances between source rocks and croplands. By 2060-2070, lowest costs (£75-

100 t<sup>-1</sup> CO<sub>2</sub>) occur in the north-east of England, the midlands and Scotland, where CDR rates are highest because of favourable soil weathering environments and regional climate effects on site water balance (precipitation minus evapotranspiration).

Nations committing to net-zero targets require carefully designed economic and policy frameworks to incentivize uptake and cover the costs of CDR technologies<sup>13,21</sup>, as well as modification of existing emissions trading schemes. Costs might be met in the near-term through farming subsidies; agriculture is heavily supported in most countries worldwide<sup>13</sup>. Actions for enhancing soil carbon storage are already subsidized in the USA, and European proposals for incentivize CDR by farmers are underway<sup>32</sup>. Redesigned agricultural policies in the UK post-Brexit aim to provide public funding to support farmers in delivering environmental public goods and contribute to net zero<sup>33</sup> by 2050. Identifying strategic options, such as ERW, with multiple co-benefits for agricultural productivity, and the environment, is key to enhancing uptake.

### **Co-benefits of ERW for agriculture**

Arable soils are a critical resource supporting multiple ecosystem services and adoption of ERW into current agricultural practices can enhance soil functions. We quantify three major soil-based co-benefits with potential to increase the demand for early deployment of the technology: reducing excess soil acidity, increasing the primary supply of fertilizer-based mineral nutrients (phosphorus, P, and potassium, K)<sup>5,9,10</sup>, and mitigating soil N<sub>2</sub>O fluxes<sup>14</sup>.

Soil acidity (i.e., pH below 6.5)<sup>34</sup> limits yields and correction is essential for good soil management, crop growth, nutrient use efficiency and environmental protection<sup>35</sup>. Following initialization with topsoil (0-15 cm) pH values based on high resolution field datasets (Methods), implementation of ERW reduces the fraction of arable soils with pH less than 6.5 in England to 13% by 2035 (S1), and completely by 2045 and 2055 in S2 and S3, respectively (**Fig. 5a**). In Scotland, where agricultural soils are more acidic than in England, the co-benefit of ERW in raising soil pH could be considerable, with reductions to 10% by 2050 in S1 and eliminating acidic soils by 2045-2050 in S2 and S3 (**Fig. 5b**). Reversing soil acidification across England and Scotland can increase nutrient uptake to boost yields on underperforming croplands<sup>34,35</sup>, lower the potential for metal toxicity<sup>10</sup> at low pH, and enhance nitrogen fixation by legumes<sup>36</sup>. Additionally, calcium released by ERW can stimulate root growth and water uptake<sup>37</sup> and multi-element basalt can fortify staple crops like cereals with important micronutrients including iron and zinc<sup>9</sup>. Raising soil pH with



widespread ERW practices in the UK, and elsewhere, to improve agricultural productivity<sup>38</sup>, releases land for additional CDR opportunities, including afforestation, and bioenergy cropping<sup>4,21</sup>.

Calculated rates of inorganic P and K nutrient supply for crops via ERW of basalt are comparable to typical P and K fertilizer application rates for major tillage crops (Extended Data Fig. 9). ERW with basalt could therefore substantially reduce the reliance of agriculture on expensive and finite rock-derived sources of P and K fertilizers required to support increased agricultural production over the next 50 years in the UK, and globally, to meet the demands of a growing human population<sup>39</sup>. Reductions in P- and K- fertilizer usage lower unintended environmental impacts, supply chain CO<sub>2</sub> emissions and costs. For the UK, assuming annual fertilizer application on ERW cropland areas in S1-S3 to replenish pools of P and K being removed, avoided carbon emissions are estimated to be 0.1 to 1 Mt CO<sub>2</sub> yr<sup>-1</sup>, with maximum cost savings of £100-700 million yr<sup>-1</sup> by 2070 (**Fig. 5, c-f**). These savings could contribute to offsetting the cost of undertaking ERW practices, but would be reduced by precision farming techniques, including applying variable levels of fertilisers within fields, and controlled release fertilisers.

Practices that optimise the efficient use of nitrogen on croplands to reduce N<sub>2</sub>O emissions from soils are important for ambitious net-zero agriculture pathways in the UK<sup>4</sup>. Our process-based model simulations, calibrated with field data<sup>14</sup>, indicate ERW deployment on UK croplands could reduce soil N<sub>2</sub>O emissions by ~0.1 Mt CO<sub>2equilvanet</sub> yr<sup>-1</sup>, ~1 Mt CO<sub>2equilvanet</sub> yr<sup>-1</sup>, and ~1.5 Mt CO<sub>2equilvanet</sub> yr<sup>-1</sup> by 2070 in S1 to S3, respectively (**Fig. 5e**); equivalent to up to a 20% reduction relative to croplands in 2010 (**Fig. 5f**). This contrasts with large-scale land-based CDR strategies for increasing soil organic carbon stocks which can increase soil N<sub>2</sub>O emissions<sup>40</sup>. ERW may therefore offer a new management option for mitigating soil N<sub>2</sub>O fluxes comparable in magnitude to other proposed abatement measures<sup>41</sup> with the additional win of CDR.

### **Societal and community acceptability**

Societal acceptance of ERW practices is needed from the national-political to local community and individual farm scales. ‘Acceptance’ in this context should be regarded not as an absolute mandate to proceed, but rather recognizing the need to work with stakeholders and affected publics to identify the conditions under which this technology might proceed<sup>42</sup>. Additional mining operations with unintended environmental impacts raise particular sensitivities<sup>42</sup> and two of our scenarios (S2 and S3) require new mines between 2035 and 2050 to provide basalt; increases post-2035 account for delays due to complex licensing procedures (Extended Data Fig. 4). Concentrating resource

production at larger sites ( $\sim 1$  Mt basalt  $\text{yr}^{-1}$ ) requires annual increases in mine number of 6% (S2) and 13% (S3); smaller mines ( $\sim 250$  kt  $\text{yr}^{-1}$ ) necessitate larger annual increases (Supplementary Information). However, the scale-up rate is less than the historical 10-year maximum (1960-1970) and limited to 15 years. Recycling the UK's annually produced calcium silicate construction and demolition waste ( $\sim 80$  Mt  $\text{yr}^{-1}$ )<sup>43</sup>, which has potential to substitute for basalt<sup>6</sup>, could reduce substantially mined resource demand by between 80% (S2) and 45% (S3).

Traditional mining operations provide local employment opportunities but have encountered controversy nonetheless because of concerns about sustainability, community impacts and local health and environmental risks<sup>44</sup>. Mining operations to enhance national carbon sequestration may raise somewhat different ethical and risk-benefit narratives<sup>45</sup>. Procedural and distributional fairness in siting mines, alongside long-term proactive engagement with communities likely to be affected by any new mining operations, will be critical for acceptance<sup>44</sup>, together with sustainable management plans for quarry restoration post-extraction<sup>46,47</sup>. The issue of mining new materials for CDR is part of a wider debate regarding the sustainability of increasing resource extraction for green technologies, such as electric vehicles or photo-voltaic cells. Achieving this at scale requires development of innovative solutions combining improved resource efficiency and use of waste mining products, circular economy production systems, and extraction efforts focused primarily in the regions or countries where materials are to be used<sup>48</sup>. Although nature-based techniques for CDR (e.g. forestry, carbon sequestration in soils) are likely to be preferred by public groups over engineered technologies<sup>42,49</sup>, they are unlikely to be sufficient to deliver net-zero nationally or globally. Above all, broad societal support is unlikely to be forthcoming unless ERW is developed alongside an ambitious portfolio of conventional climate mitigation policies<sup>49</sup>.

### **Implications for ERW deployment**

Our analysis with dynamic ERW carbon budget modelling suggests this technically straightforward CDR technology to implement could prove transformative for utilizing agriculture to mitigate climate change<sup>6,9,10</sup> and play a larger role in national CDR portfolio programmes than previously realized. Unlike industrial CDR processes, including BECCS or DACCS, ERW may be rolled out without major new industrial infrastructure, incentivised through amended agricultural subsidy frameworks. We show that eliminating the energy-demanding requirement for milling rocks to fine particle sizes requires early and sustained implementation of ERW practices, subject to public acceptance. This has the additional important advantages of maximising CDR and lowering costs

to a highly competitive price of £80-110 t<sup>-1</sup> CO<sub>2</sub> yr<sup>-1</sup> by 2070. Our findings underscore the urgent need for long-term field trials across a range of agricultural systems to evaluate this technology with empirical evidence, alongside monitoring of potential unintended negative consequences<sup>9,50</sup>. High-resolution geospatial ERW assessments provide a detailed basis for mapping out routes to technological development and afford opportunities to minimize social and economic barriers by identifying priority regions for public engagement. Scaling up ERW in the UK and other G20 nations will require funding, public support, regulation and governance to ensure sustainability, and a stable policy framework<sup>4,13</sup> to accelerate global CDR goals with agriculture<sup>6,9,10</sup> as the world transitions to net-zero.

### **Acknowledgements**

We thank Corrine Le Quéré, Adrian Collins, Rob Freckleton, Jonathan Leake and Jonathan Scurlock for comments on an earlier draft. We gratefully acknowledge funding of this research with a Leverhulme Research Centre Award (RC-2015-029; D.J.B.) from the Leverhulme Trust. D.J.B. and P.R. acknowledge UKRI funding under the UK Greenhouse Gas Removal Programme (BB/V011359/1, DJB; NE/P019943/1, NE/P019730/1, P.R.). M.V.M. acknowledges funding from the UKRI Future Leaders Fellowship Programme (MR/T019867/1). We acknowledge the high-performance computing support from Cheyenne ([doi:10.5065/D6RX99HX](https://doi.org/10.5065/D6RX99HX)) provided by NCAR's Computational and Information Systems Laboratory, sponsored by the National Science Foundation. We acknowledge the World Climate Research Programme's Working Group on Coupled Modelling responsible for CMIP and thank the climate modelling groups for producing and making available their model output. For CMIP the US Department of Energy's Program for Climate Model Diagnosis and Intercomparison provides coordinating support and led development of software infrastructure in partnership with the Global Organization for Earth System Science Portals.

### **Author contributions**

D.J.B., E.P.K., M.V.M., M.R.L., P.R. and S.A.B. designed the study, E.P.K., M.V.M and M.R.L. undertook model development, simulations and coding, with input from L.L.T., S.A.B. and D.J.B. E.P.K. undertook data analysis and synthesis, R.M.E. undertook the UK transport analyses with input from L.K., P.R. developed the silicate supply scenarios, A.L. undertook the X-ray diffraction analyses of UK basalts, and N.P. wrote sections on public perception. N.V. and P.B.H. undertook the GENIE analyses, J.-F.M., H.P., P.V.V., N.R.E. and P.B.H. provided analyses and data on UK

national economics, energy production, and CO<sub>2</sub> emissions. L.L.T. led drafting the Supplementary Information section. D.J.B. and S.A.B. wrote the manuscript with input from co-authors.

### **Competing Interests**

The authors declare no competing interests.

## Figure legends

**Figure 1 | Net carbon dioxide removal by enhanced rock weathering deployed with UK arable croplands.** Panels (a), (b) and (c) display simulated net carbon dioxide removal (CDR) and for low- (S1), medium- (S2), and high- (S3) resource extraction scenarios, respectively, and annual basalt extracted (dashed line). Results are shown for two particle size distributions ( $p_{80} = 10 \mu\text{m}$  diameter and  $p_{80} = 100 \mu\text{m}$  diameter;  $p_{80} = 80\%$  of particles  $\leq$  specified value). Shaded area denotes 95% confidence limits. Panels (d), (e) and (f) display iso-lines of UK decadal running-average net CDR ( $\text{Mt CO}_2 \text{ yr}^{-1}$ ) for the three resource extraction scenarios over time (2020-2070). Panels (a) to (f) are mean results for three UK-specific basalts. Panels (g), (h) and (i) display cumulative net CDR over time for low-, medium- and high-resource extraction scenarios by UK region, respectively; mean of simulations with  $p_{80} = 10$  and  $100 \mu\text{m}$  and three UK-specific basalts.

**Figure 2 | Mapped fine-scale decadal average UK net carbon dioxide removal.** Mapped net carbon dioxide removal by enhanced rock weathering deployed on arable croplands for (a) low- (S1), (b) medium- (S2) and (c) high- (S3) resource extraction scenarios. Mean of simulations with two  $p_{80}$ s (10 and  $100 \mu\text{m}$ ) and three UK-specific basalts.

**Figure 3 | Costs of carbon dioxide removal by enhanced rock weathering deployed with UK arable croplands.** Panels (a), (b) and (c) display costs of net carbon dioxide removal for low- (S1) medium- (S2) and high- (S3) resource extraction scenarios, respectively, over time (2020-2070). Results are shown for two particle size distributions ( $p_{80} = 10 \mu\text{m}$  diameter and  $p_{80} = 100 \mu\text{m}$  diameter). Shaded area denotes 95% confidence limits. Panels (d), (e) and (f) show the breakdown between ERW processes contributing to CDR costs, including savings resulting from basalt substituting for phosphorus (P) and potassium (K) fertilizers averaged for 2060-2070. Errors indicate 95% confidence limits. All panels display average results for three UK-specific basalts.

**Figure 4 | Mapped fine-scale decadal average UK net carbon dioxide removal costs.** Mapped net carbon dioxide removal costs by enhanced rock weathering deployed on arable croplands for (a) low- (S1), (b) medium- (S2) and (c) high- (S3) resource extraction scenarios. Mean of simulations with two  $p_{80}$ s (10 and  $100 \mu\text{m}$ ) and three UK-specific basalts.

**Figure 5 | Agricultural ecosystem co-benefits of enhanced rock weathering.** Reduction in the fraction of acidic land in (a) England and (b) Scotland following deployment of ERW,  $\text{CO}_2$

emissions avoided (**c**) and cost savings (**d**) resulting from using basalt to substitute for phosphorous (P) and potassium (K) fertilizers. Panel (**e**) and (**f**) display soil N<sub>2</sub>O emission reductions from croplands (as CO<sub>2</sub> equivalents), and percentage change from 2010, following ERW deployment. N<sub>2</sub>O results are shown as 10-yr annual running averages. Results are shown for low- (S1), medium- (S2) and high- (S3) resource extraction scenarios in all panels, with for two particle size distributions ( $p_{80} = 10 \mu\text{m}$  diameter and  $p_{80} = 100 \mu\text{m}$  diameter). Shaded areas denote 95% confidence limits.

## References

1. <https://climateaction.unfccc.int/views/cooperative-initiative-details.html?id=94>
2. Hansen, J. *et al.* Assessing “dangerous climate change”: required reduction of carbon emissions to protect young people, future generations and nature. *PLoS ONE* **8**, e81648 (2013).
3. HM Government. *Greenhouse gas removals – Call for evidence* (HMG, London, pp. 1-35, 2020).
4. Committee on Climate Change. *The sixth carbon budget. The UK’s path to net zero.* (Committee on Climate Change, London, pp.1-448, 2019).
5. Hartmann, J. *et al.* Enhanced chemical weathering as a geoengineering strategy to reduce atmospheric carbon dioxide, supply nutrients, and mitigate ocean acidification. *Rev. Geophys.* **51**, 113–149 (2013).
6. Beerling, D.J. *et al.* Potential for large-scale CO<sub>2</sub> removal via enhanced rock weathering with croplands. *Nature* **583**, 242-248 (2020).
7. Kohler, P., Hartman, J. & Wolf-Gladrow, D.A. Geoengineering potential of artificially enhanced silicate weathering of olivine. *Proc. Natl Acad. Sci. USA* **107**, 20228–20233 (2010).
8. Taylor, L.L. *et al.* Enhanced weathering strategies for stabilizing climate and averting ocean acidification. *Nat. Clim. Change* **6**, 402–406 (2016).
9. Beerling, D.J. *et al.* Farming with crops and rocks to address global climate, food and soil security. *Nat. Plants* **4**, 138-147 (2018).
10. Kantola, I. B. *et al.* Potential of global croplands and bioenergy crops for climate change mitigation through deployment for enhanced weathering. *Biol. Lett.* **13**, 20160714 (2017).
11. Kelland, M.E. *et al.* Increased yield and CO<sub>2</sub> sequestration potential with the C<sub>4</sub> cereal *Sorghum bicolor* cultivated in basaltic rock dust-amended agricultural soil. *Global Change Biol.* **26**, 3658-3676 (2020).
12. Vakilifard, N. *et al.* The role of enhanced weathering deployment with agriculture in limiting future warming and protecting coral reefs. *Environ. Res. Lett.* **19**, 094005 (2021).
13. Cox, E. & Edwards, N.R. Beyond carbon pricing: policy levers for negative emissions technologies. *Clim. Policy* **19**, 1144-1156 (2019).
14. Blanc-Betes, E. *et al.* In silico assessment of the potential of basalt amendments to reduce N<sub>2</sub>O emissions from bioenergy crops. *Global Change Biol. Bioen.* **13**, 224-241 (2021).

15. Reay, D.S. *et al.* Global agriculture and nitrous oxide emissions. *Nat. Clim. Change* **2**, 410–416 (2012).
16. Bhunoo, R. & Poppy, G.M. A national approach for transformation of the UK food system. *Nat. Food* **1**, 6–8 (2020).
17. Holden, P.B. *et al.* Climate-carbon cycle uncertainties and the Paris Agreement. *Nat. Clim. Change* **8**, 609–613 (2018).
18. Renforth, P. The potential of enhanced weathering in the UK. *Int. J. G. Gas. Cont.* **10**, 229–243 (2012).
19. Smith, P., Haszeldine, R.S. & Smith, S.M. Preliminary assessment of the potential for, and limitations to, terrestrial negative emissions technologies in the UK. *Environ. Sci. Processes & Impacts*, **18**, 1400 (2016).
20. The Royal Society-Royal Academy of Engineering. *Greenhouse gas removal technologies* (The Royal Society, London, 2018).
21. IPCC. *Global warming of 1.5°C. An IPCC Special Report on the impacts of global warming of 1.5°C above pre-industrial levels and related global greenhouse gas emission pathways* (World Meteorological Organization, Geneva, Switzerland, 2018).
22. Moosdorf, N., Renforth, P. & Hartmann, J. Carbon dioxide efficiency of terrestrial weathering. *Environ. Sci. Tech.* **48**, 4809–4816 (2014).
23. Hartmann, J. & Amann, T Limits of weathering potentials – deductions from column experiments. *Goldschmidt* 2021, <https://2021.goldschmidt.info/goldschmidt/2021/meetingapp.cgi/Paper/6179>
24. Fletcher, T.I. *et al.* The carbon sequestration potential of Scottish native woodland. *Environ. Res. Commun.* **3**, 041003 (2021).
25. Friggens, N.L. *et al.* Tree planting in organic soils does not result in net carbon sequestration on decadal timescales. *Glob. Change Biol.* **26**, 5178–5188 (2020).
26. Bradfer-Lawrence, T. *et al.* The potential contribution of terrestrial nature-based solutions to a national ‘net zero’ climate target. *J. Appl. Ecol.* doi: 10.1111/1365-2664.14003 (2021).
27. Powlson, D.S., *et al.* Limited potential of no-till agriculture for climate change mitigation. *Nature Clim. Change* **4**, 678–683 (2014).
28. Ostle, N.J., Levy, P.E., Evans, C.D. & Smith, P. UK land use and soil carbon sequestration. *Land Use Policy* **26S**, S274–S283 (2009).
29. Poeplau, C. & Don, A. Carbon sequestration in agricultural soils via cultivation of cover crops – a meta-analysis. *Agri. Ecosys. Environ.* **200**, 33–41 (2015).



30. Zamanian, K., Pustovoytov, K., & Kuzyakov, Y. Pedogenic carbonates: forms and formation processes. *Earth Sci. Rev.* **157**, 1–17 (2016).
31. <https://ahdb.org.uk/GB-fertiliser-prices>
32. Schenuit, F. *et al.* Carbon dioxide removal policy in the making: assessing developments in 9 OECD cases. *Front. Clim.* **3**, article 638805, (2021).
33. Clements, J. *et al.* How can academic research on UK agri-environmental schemes pivot to meet the addition of climate mitigation aims? *Land Use Policy* **106**, 105441(2021).
34. Goulding, K.W.T. Soil acidification and the importance of liming, agricultural soils with particular reference to the United Kingdom. *Soil Use Manag.* **32**, 390-399 (2016).
35. Holland, J.E. *et al.* Liming impacts on soils, crops and biodiversity in the UK: a review. *Sci. Tot. Environ.* **610-611**, 316-332 (2018).
36. Alves, L.A. *et al.* Biological N<sub>2</sub> fixation by soybeans grown with and without liming on acid soils in a no-till integrated crop-livestock system. *Soil Till. Res.* **209**, 104923 (2021).
37. Lynch, J.P. & Wojciechowski, T. Opportunities and challenges in the subsoil: pathways to deeper rooted crops. *J. Exp. Bot.* **66**, 2199-2210 (2015).
38. Lerhmann, J. & Possinger, A. Atmospheric CO<sub>2</sub> removal by rock weathering. *Nature* **583**, 205-205 (2020).
39. Amundson, R. *et al.* Soil and human security in the 21<sup>st</sup> Century. *Science* **348**, 126107-1 (2015).
40. Guenet *et al.* Can N<sub>2</sub>O emissions offset the benefits from soil organic carbon storage? *Glob. Change Biol.* **27**, 237-256 (2020).
41. Rees, R.M. *et al.* Nitrous oxide mitigation in UK agriculture. *Soil Sci. Plant Nutr.* **59**, 3-15 (2013).
42. Cox, E., Spence, E. & Pidgeon, N. Public perceptions of carbon dioxide removal in the United States and the United Kingdom. *Nature Clim. Change* **10**, 744-749 (2020).
43. Department for Communities and Local Government. *Survey of arisings and use of alternatives to primary aggregates in England. Construction, demolition and excavation waste* (Crown Estates, London, 2007).
44. Moffat, K. *et al.* In: Lodhia, S. (Ed.), *Mining and Sustainable Development: Current Issues*. (Routledge, London, pp. 45–62, 2018).
45. Cox E., Pidgeon N.F., Spence E.M. & Thomas, G. Blurred lines: The ethics and policy of greenhouse gas removal at scale. *Front. Environ. Sci.* **6**, article 38 (2018).

46. Bradshaw, A. Restoration of mined lands—using natural processes. *Ecol. Eng.* **8**, 255-269 (1997).
47. Novak, J. & Prach, K. Vegetation succession in basalt quarries: pattern on a landscape scale. *App. Veg. Sci.*, **6**, 111-116 (2003).
48. Herrington, R. Mining our green future. *Nat. Rev. Materials* **6**, 456-458 (2021).
49. Wolske, K.S. *et al.* Public support for carbon dioxide removal strategies: the role of tampering with nature perceptions. *Clim. Change* **152**, 345–361 (2019).
50. Edwards, D.P. *et al.* Climate change mitigation: potential benefits and pitfalls of enhanced rock weathering in tropical agriculture. *Biol. Lett.* **13**, 20160715 (2017).

## Methods

**Resource Extraction Scenarios.** Scenario 1 (S1, low supply): per capita production of aggregate continues to fall from 1.9 to 1.5 t yr<sup>-1</sup> by 2032 and remains constant thereafter, with the spare capacity used and ramped up for ERW. Scenario 2 (S2, medium supply): rock extraction is scaled by 7% (half the historical maximum rate of increase) until total additional capacity is equal to the maximum historical value in 1990 (100 Mt yr<sup>-1</sup>), and Scenario 3 (S3, high supply): rock extraction is scaled by 15% (i.e., historical annual 10-year rolling average) until the additional capacity is 160 Mt yr<sup>-1</sup>; i.e., equivalent to the total increase in UK crushed rock supply post-1945 (Supplementary Information). Extraction of resources scales at rates compatible with historical patterns (Extended Data Fig. 4) and those advanced for delivering CDR by BECCS, and its supply chains, and DACCS<sup>4</sup>.

**Soil Profile ERW Modelling.** Our analysis uses a 1-D vertical reactive transport model for rock weathering with steady-state flow and transport through a series of soil layers. The transport equation includes a source term representing rock grain dissolution within the soil profile<sup>4</sup> with significant advancements to incorporate the effects of the biogeochemical transformations of nitrogen fertilizers (Supplementary Information). The core model accounts for changing dissolution rates with soil depth and time as grains dissolve, and chemical inhibition of dissolution as pore fluids approach equilibrium with respect to the reacting basaltic mineral phases, and the formation and dissolution of pedogenic calcium carbonate mineral in equilibrium with pore fluids<sup>4</sup>. Simulations consider UK basalts with specified mineralogy from three commercial quarries (Supplementary Information).

We model ERW of a defined particle size distribution (psd) with the theory developed previously<sup>4</sup>. As the existing psds at each soil layer are at different stages of weathering, the combined psd at each level, and for each mineral, is calculated and tracked over time<sup>4</sup>. We account for repeated basalt applications by combining the existing psd with the psd of the new application. Simulated mineral dissolution fluxes from the model output were used to calculate the release of P and K over time. Mass transfer of P within the relatively more rapidly dissolving<sup>51</sup> accessory mineral apatite is calculated based on the P content of the rock and the volume of bulk minerals dissolved during each time step.

The mathematical model combines a multi-species geochemical transport model with a mineral mass balance and rate equations for the chemical dissolution of basaltic mineral phases. The model includes an alkalinity mass balance that includes the effect of fertiliser applications and soil N

cycling and dynamic calculation of pH in soil pore waters. The main governing equations are the following.

**Transport equation.** The calculated state variable in the transport equation is the dissolved molar equivalents of elements released by stoichiometric dissolution of mineral  $i$ , in units of mole  $L^{-1}$ .  $\phi$  is volumetric water content,  $C_i$  is dissolved concentration (mole  $L^{-1}$ ) of mineral  $i$  transferred to solution,  $t$  is time (mths),  $q$  is vertical water flux (mth  $y^{-1}$ ),  $z$  is distance along vertical flow path (m),  $R_i$  is the weathering rate of basalt mineral  $i$  (mole per litre of bulk soil  $mth^{-1}$ ) and  $C_{eq_i}$  is the solution concentration of weathering product at equilibrium with the mineral phase  $i$  (Equation 1). Values for  $C_{eq}$  for each of the mineral phases in the basalt grains by calibrating the results of the performance model against those of a 1-D reactive transport model, as described previously<sup>4</sup>.

Rates of basalt grain weathering define the source term for weathering products and are calculated as a function of soil pH, soil temperature, soil hydrology, soil respiration and crop net primary productivity (NPP). The vertical water flux is zero when pore water content is below a critical threshold for vertical flow. Weathering occurs under no-flow conditions and the accumulated solutes in pore water are then advected when water flow is initiated under sufficient wetting, tracked using a single bucket model.

$$\phi \frac{\partial C_i}{\partial t} = -q \frac{\partial C_i}{\partial z} + R_i \left( 1 - \frac{C_i}{C_{eq_i}} \right) \text{ (Eq. 1)}$$

**Mineral mass balance.** The change in mass of basalt mineral  $i$ ,  $B_i$ , is defined by the rate of stoichiometric mass transfer of mineral  $i$  elements to solution. Equation 2 is required because we are considering a finite mass of weathering rock, which over time can react to completion, either when solubility equilibrium between minerals and pore water composition is reached, or when applied basalt is fully depleted.

$$\frac{\partial B_i}{\partial t} = -R_i \left( 1 - \frac{C_i}{C_{eq_i}} \right) \text{ (Eq. 2)}$$

**Removal of weathering products.** The total mass balance over time (Equation 3) for basalt mineral weathering allows calculation of the products transported from the soil profile. The total mass of weathering basalt is defined as follows where  $m$  is the total number of weathering minerals in the rock,  $t_f$  is the duration of weathering and  $L$  is the total depth of the soil profile (m). We define  $q$  as the net monthly sum of water gained through precipitation and irrigation, minus evapotranspiration, as calculated by CLM5.

$$\text{Total weathered Basalt} = \sum_{i=1}^m \phi \int_{z=0}^L C_i(t, z) dz + q \int_{t=0}^{t_f} C_i(t, L) dt \text{ (Eq. 3)}$$

**Coupled Climate-C-N cycle ERW Simulations.** Our model simulation framework (**Extended Data Fig 1**) starts with future UK climates (2020-2070) from the medium-mitigation future pathway climate (SSP3-7.0) ensemble of CMIP6 runs with the Community Earth System Model v.2. Future climates were used to drive the Community Land Model v.5 (CLM5) to simulate at high spatial resolution (23 km × 31 km) and temporal (30 min) resolution terrestrial carbon and nitrogen cycling with prognostic crop growth and other ecosystem processes, including heterotrophic respiration<sup>52,53</sup> (Supplementary Information). CLM5 simulates monthly crop productivity, soil hydrology (precipitation minus evapotranspiration), soil respiration and nitrogen cycling. CLM5 has representation of eight crop functional types, each with specific ecophysiological, phenological and biogeochemical parameters<sup>52,53</sup>. CLM5 includes CO<sub>2</sub> fertilization effects on agricultural systems benchmarked against experiments and observations<sup>54,55</sup>. Atmospheric CO<sub>2</sub> increase of ~200 ppm from 2015 to 2070, as defined by SSP3-7.0. In our CLM5 simulations with rising CO<sub>2</sub> and climate change, wheat NPP increased by 8%, evapotranspiration (Et) decreased by 21% and water-use efficiency increased by 25% (Supplementary Information). Both increasing NPP and decreasing Et can facilitate weathering in our soil profile ERW model (Supplementary Information). We initialized CLM5 simulations for 2010 using fully spun-up conditions from global runs at ~100 km × 100 km resolution, adding an extra 60-year spin-up in the regional set-up to stabilize the CN pools to the higher resolution setting.

CLM5 includes an interactive nitrogen fertilization scheme that simulates fertilization by adding nitrogen directly to the soil mineral nitrogen pool to meet crop nitrogen demands using both synthetic fertilizer and manure application<sup>52,53</sup>. Synthetic fertilizer application is prescribed by crop type and varies spatially for each year based on the Land Use Model Intercomparison Project and land cover change time series (LUH2 for historical and SSP3 for future)<sup>55,56</sup>. N-fertilizer rates increase by 18% per decade from 2020 to 2050 in agreement with the UK's Committee on Climate Change forecasts of future N-fertilizer usage<sup>57</sup>, and then stabilise from 2050 to 2070. Average UK CLM5 fertilizer application rates (148 kg N ha<sup>-1</sup>yr<sup>-1</sup>) are consistent with current practices<sup>58</sup>. Organic fertilizer is applied at a fixed rate (20 kg N ha<sup>-1</sup>yr<sup>-1</sup>) throughout the simulations.

CLM5 tracks nitrogen content in soil, plant, and organic matter as an array of separate nitrogen pools and biogeochemical transformations, with exchange fluxes of nitrogen between these pools<sup>52,53</sup>. The model represents inorganic N transformations based on the DayCent model, which includes separate dissolved NH<sub>4</sub><sup>+</sup> and NO<sub>3</sub><sup>-</sup> pools, as well as environmentally controlled nitrification,

denitrification and volatilization rates<sup>59</sup>. To model the effect of basalt addition on fluxes of N<sub>2</sub>O from soil, we included the updated denitrification DayCent module<sup>14</sup>, modified to capture the soil pH ranges in UK croplands. The possible effect of increased soil pH from basalt application increasing NH<sub>3</sub> volatilization and, indirectly, N<sub>2</sub>O emissions, is not explicitly modelled. However, the small error term is likely small, given it accounts for less than 5% of total agricultural N<sub>2</sub>O emissions<sup>60,61</sup>. Cropland CLM5 soil nitrogen emissions are within the range of estimates in UK croplands based on bottom-up inventories and other land surface models, with N<sub>2</sub>O fluxes showing broad similarities in terms of regional patterns and magnitude with the UK National Atmospheric Emission Inventory (Supplementary Information).

**Modelling Soil Nitrogen Effects on ERW.** A significant theoretical advance over previous modelling is the inclusion of mechanistic simulation of nitrogen cycling processes coupled to ERW via sixteen stoichiometric nitrogen transformations that influence the soil weathering environment (Supplementary Information). The modelling accounts for 20 depths (20 soil layers) in the soil profile at each location with a monthly time-step; Supplementary Information gives the variables passed from CLM5 by time and depth to the 1-D ERW model. At each depth, we compute nitrogen transformation effects on soil water alkalinity with reaction stoichiometries that add or remove alkalinity. Together with soil CO<sub>2</sub> levels, this affects pore water pH and the aqueous speciation that determines mineral weathering rates. This modelling advance allows us to mechanistically account for the impact of N fertilisation, recognised to potentially lead to nitric acid dominated weathering<sup>62,63</sup> at low pH with no carbon capture, of cropland on basalt weathering rates. Dynamic modelling at monthly time-steps resolves seasonal cycles of CDR via alkalinity fluxes and soil carbonate formation/dissolution in response to future changes in atmospheric CO<sub>2</sub>, climate, land surface hydrology, and crop and soil processes.

The effect of the nitrogen cycle on the soil acidity balance (Extended Data Figure 3) is derived from nitrogen transformations associated with the production or consumption of hydrogen ions (Supplementary Information). We assigned a stoichiometric acidity flux  $\Delta H_{i,N}$  (mol H<sup>+</sup> mol<sup>-1</sup> N) to each nitrogen flux  $F_{i,N}$  (gN m<sup>-3</sup>soil s<sup>-1</sup>) calculated by the CLM5 code (Supplementary Information). The product ( $F_{i,N} \cdot \Delta H_{i,N}$ ), with appropriate unit conversions, gives the acidity flux during the time-step  $\Delta t$  (s month<sup>-1</sup>) for the  $i^{\text{th}}$  reaction of the CLM5 nitrogen cycle. Their sum (Eq 4) is, therefore, the total change in acidity  $\Delta \text{Acidity}_N$  due to the CLM5 nitrogen cycle:

$$\Delta \text{Acidity}_N = \sum (F_{i,N} \Delta H_{i,N}) / 14.0067 \Delta t \quad (\text{Eq. 4})$$

where  $14.0067 \text{ gN mol}^{-1} \text{ N}$  is the atomic weight of nitrogen and the time-step is one month. Along with the Ca, Mg, K, and Na ions released from weathering the applied minerals,  $\Delta\text{Acidity}_N$  contributes a negative term to the soil water alkalinity balance used to calculate the soil pH<sup>4</sup>.

$$\text{Alk}_t = \text{Alk}_{t-1} + 2 \cdot (\text{Ca}_{\text{weath}} + \text{Mg}_{\text{weath}}) + \text{K}_{\text{weath}} + \text{Na}_{\text{weath}} - \Delta\text{Acidity}_N \quad (\text{Eq. 5})$$

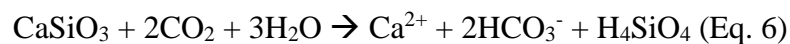
This pH value is one component that is accounted for in the rate laws for mineral dissolution and therefore influences the net alkalinity that is produced at each depth within the soil profile, and that contributes to CDR<sup>4</sup>.

The initial alkalinity profile in each grid cell is determined from the starting soil pH and the  $\text{PCO}_2$  profile at steady-state based on spin-up of the model with average long-term biomass production and soil organic matter decomposition that reflects the long-term land use history of a particular location. Alkalinity mass and flux balance for an adaptive time-step accounts for alkalinity and acidity inputs from 1) mineral dissolution rates and secondary mineral precipitation (pedogenic carbonate), 2) biomass production and decomposition<sup>64</sup> and 3) biogeochemical N transformations. The soil pH profile is determined from an empirical soil pH buffering capacity<sup>65</sup> relating soil pH to the alkalinity at each depth. The soil  $\text{PCO}_2$  depth profile of a grid cell is generated with the standard gas diffusion equation<sup>66</sup>, scaled by monthly soil respiration from CLM5. At any particular location, the soil solution is in dynamic equilibrium with dissolved inorganic carbon species and the values of gas phase soil and atmospheric  $\text{PCO}_2$ . The relative change induced by weathering will be the consumption of  $\text{H}^+$  and the production of  $\text{HCO}_3^-$ .

Using this modelling framework (Extended Data Fig. 1), we analysed a baseline application rate of  $40 \text{ t ha}^{-1} \text{ yr}^{-1}$  (equivalent to a  $<2 \text{ mm}$  layer of rock powder distributed on croplands) to UK croplands. Similar road transport of mass occurs in reverse during grain transport from field to market during UK harvest<sup>67</sup>, indicating appropriate capacity of rural transport networks to move basalt to the fields for ERW.

**Gross CDR calculations.** Gross CDR by ERW of crushed basalt applied to soils is calculated as the sum of two pathways: 1) the transfer of weathered base cations ( $\text{Ca}^{2+}$ ,  $\text{Mg}^{2+}$ ,  $\text{Na}^+$  and  $\text{K}^+$ ) from soil drainage waters to surface waters that are charge balanced by the formation of  $\text{HCO}_3^-$  ions and transported to the ocean (equation 6), and 2) formation of pedogenic carbonates (equation 7).

Pathway 1 for calcium ions:



Pathway 2 for calcium carbonate formation:



CDR, via pathway 1, potentially sequesters two moles of CO<sub>2</sub> from the atmosphere per mole of divalent cation. However, ocean carbonate chemistry reduces the efficiency of CO<sub>2</sub> removal to an extent depending on ocean temperature, salinity and the surface ocean dissolved CO<sub>2</sub> concentration. We used annual ERW alkalinity flux time series (2020-2070) calculated with our 1-D ERW model for scenarios 1 to 3 as inputs to GENIE (version 2.7.7)<sup>68,69</sup>. GENIE is an intermediate complexity Earth System Model with ocean biogeochemistry and allows computation of oceanic CDR via pathway 1. We used the same methodology as described previously<sup>12</sup> to simulate atmospheric CO<sub>2</sub> removal via release of enhanced weathering alkalinity products into the ocean. Uncertainty for each scenario was determined by ensemble GENIE simulations with 86 different parameter sets that vary 28 parameters, each calibrated to simulate a reasonable preindustrial and historical transient climate and carbon cycle<sup>68-70</sup>. CDR via pathway 2 occurs if dissolved inorganic carbon derived from atmospheric CO<sub>2</sub> precipitates as pedogenic carbonate, and sequesters 1 mol of CO<sub>2</sub> per mole of Ca<sup>2+</sup>.

### **Costs and carbon emissions of logistical operations.**

**Mining.** Breakdown of mining costs in £/t of rock for the year 2010 and a representative granite mine of 1.5k daily/375k annual output were obtained from a comprehensive analysis of UK aggregate mining<sup>71</sup>. Capital expenditure costs (CAPEX) amounted to £24,395,636 over a 50-year life cycle (£1.30/t rock) while operating expenses (OPEX) amounted to £1,150,072 per year (£3.07/t rock) for a total £4.37/t rock for the year 2010. To obtain cost projections over 2020-2070, the contribution of wages, diesel fuel and electricity consumption in OPEX (35.9%, 2.5% and 20.0% respectively) were normalized and projected for 2020-2070 using E3ME outputs of median wage, diesel prices and industrial electricity tariff respectively (Supplementary Information). CAPEX and the remaining OPEX (plant, buildings, equipment, tyres) costs in £/t rock remained constant over the period. Emissions of CO<sub>2</sub> eq./t rock extracted using diesel fuel and explosives were set at 4.29 kg CO<sub>2</sub> eq./t rock<sup>71</sup>. Emissions of CO<sub>2</sub> eq. per unit of electricity consumed were obtained by combining electricity requirements per tonne of rock (1.48 kWh/t rock) and projected Life Cycle Emissions (LCE) in kg CO<sub>2</sub> eq./kWh from 2020-2070.

**Grinding.** Grinding breakdown costs were obtained from Ref (18). CAPEX costs were set at £1.59/t rock while OPEX for plant, buildings and equipment at £0.97/t rock. Diesel fuel and personnel costs (£0.08/t rock and £0.85/t rock for 2010) were projected to 2020-2070 using the methodology described above. We expressed electricity consumption per tonne of rock grinded as a function of particle size, defined as *p*80, where 80% of the particles are equal to or less than a specified



diameter<sup>6</sup>. To obtain electricity costs we multiplied electricity consumption (kWh/t rock milled) by E3ME projections of the unit cost of electricity (£/kWh) and grinding emissions by multiplying electricity consumption by E3ME projections of electricity production LCE (g CO<sub>2</sub>eq/kWh).

**Spreading.** Spreading costs were set to £8.3/t rock for the year 2020 by averaging costs in the UK and USA<sup>6</sup>. Spreading costs were assigned equally to equipment, fuel/electricity and wages with E3ME data used to provide cost projections to 2070 for the last two. A sigmoid function showing transition to electric cars was obtained from E3ME, to which a 10-year lag was added to signify a delayed uptake by heavy agriculture vehicles (Supplementary Information). Spreading emissions were set to 0.003 kg CO<sub>2</sub>/t rock<sup>18</sup>. Our cost assessments assume ERW practices are undertaken on farms as part of business-as-usual land management practices. Pricing of external contracting of land management for rock dust application to soils is uncertain but could increase CDR prices per t CO<sub>2</sub> on the order of 10-15%.

**Fertilizers.** Projections of phosphorus (P) fertilizer prices (2020-2070) for a global medium resource scenario were obtained from ref 72, showing an increase in global prices due to depletion of phosphate reserves<sup>72-74</sup>. Even though potassium (K) resources are also depleting, we kept K prices constant as alternative technologies and opening of new mines in the Global South might alleviate the problem<sup>75</sup>. UK fertilizer prices for the year 2020 were used<sup>76</sup> as a baseline for our projections. Fertilizer savings were obtained as the product of release (kg) of P and K by their unit price (£/kg) over the time period 2020-2070. Life cycle assessment CO<sub>2</sub> emissions for P and K fertiliser were calculated as average values for different time horizons from the methodologies included in the Ecoinvent database<sup>77</sup> (Supplementary Information). Global Markets for these products were selected for this analysis to include all that those fertilisers coming to the UK from any region of the world.

**Energy requirements.** Electricity supply characteristics for the UK were obtained from E3ME simulations (see next section). Annual electricity supply increases from 320 GWh yr<sup>-1</sup> in 2020 to 637 GWh yr<sup>-1</sup> in 2070, with Life Cycle Emissions dropping from 177.4 gCO<sub>2</sub>/kWh to -64.5 gCO<sub>2</sub>/kWh. The electricity mix profile shows an initial transition to onshore wind energy, followed by a significant uptake of solar and various carbon capture and storage technologies.

Cost of enhanced rock weathering in £/t CO<sub>2</sub> CDR was obtained for annual from eq. 8 by summing up the logistical costs for all locations (£) that rock is applied according to each scenario for the particular year and dividing by their total net CDR (t CO<sub>2</sub>) (equation 8). Mining and

spreading costs are functions of year as the application rate is the same for all locations. Grinding costs are a function of year and p80. Transport costs are function of year and location and consider distance from the rock source. P and K release is a function of year, p80 and location, as both particle size and location (climate) affect weathering rates and subsequently elemental release. All processes costs are functions of year due to time-varying wage, fuel, electricity and fertilizer costs.

$$\begin{aligned}
 & \text{Costs}(y, p80) \\
 = & \sum_{\text{Locations}} \frac{\text{Min}(y) + \text{Grind}(y, p80) + \text{Transp}(y, loc) + \text{Spread}(y) - P(y, p80, loc) - K(y, p80, loc)}{CO_2 \text{ Gross Seq}(y, p80, loc) - CO_2 \text{ Secondary Emissions}(y, p80, loc)}
 \end{aligned}$$

(Eq. 8)

Secondary emissions (t CO<sub>2</sub>) for each location were obtained by summing the emissions of each process (t CO<sub>2</sub>/ t rock) in that year and multiplying by rock application (t rock) (equation 9)

$$\begin{aligned}
 & CO_2 \text{ Secondary Emissions}(y, p80, loc) \\
 & = [\text{Min}(y) + \text{Grind}(y, p80) + \text{Transp}(y, loc) + \text{Spread}(y) - P(y, p80, loc) \\
 & \quad - K(y, p80, loc)] \times \text{Rock}(y, loc)
 \end{aligned}$$

(Eq. 9)

An initial run determined the order of the grid cells based on their weathering potential. Rock was then applied prioritizing grid cells with the highest potential while the addition of rock in new areas each year was constrained by the annual rock availability of each scenario.

**Transportation.** Detailed transport analyses (based on UK road and rail networks) were undertaken to calculate distances costs and CO<sub>2</sub> emissions for the distribution of rock dust from source areas to croplands. We used the GLiM database for the UK distribution of basalt deposits<sup>78</sup> and the 2019 land cover map (see Drivers, below), to calculate transportation distances, cost (pound per tonne of rock dust per kilometre), and emissions (CO<sub>2</sub> tonne-kilometre<sup>-1</sup>) from potential local rock sources to cropland areas, together with UK road and rail transport networks<sup>79</sup>. Spatial analysis was undertaken with least-cost path algorithms from the ArcGIS software<sup>80</sup>.

Wages and electricity/fuel prices and CO<sub>2</sub> emission factors were derived from E3ME's 1.5 °C energy scenario<sup>1</sup>. We started using typical fuel/electricity consumption for both freight road, 2.82 km/litre and 3.07 kwh/km (ref 71) and rail, 98 km/litre (ref. 77), to estimate projected transport efficiency expressed in cost/emissions of a tonne of rock dust per kilometre (t km<sup>-1</sup>)<sup>81-83</sup>. Transport cost distribution per tonne-kilometre was derived using generic road and rail cost models that include wages, fuel, maintenance and depreciation<sup>84-85</sup>. UK rail freight diesel-to-electricity decarbonization transition is already ongoing<sup>86,87</sup>, and we used the continued projection for this

transport mode. For road freight, the transport technology transition from the E3ME for electric vehicles was adopted, modified under the assumption that diesel ban policies and the availability of electric Heavy Goods Vehicles for basalt transportation take place after 2030<sup>88</sup>.

**Energy and economic forecasts.** UK energy-economic modelling (2020-2070)<sup>89-91</sup> was based on an updated version of the scenario described in (ref.<sup>17</sup>) that includes carbon pricing and has responses for the power sector (output and efficiency) consistent with government policy<sup>92</sup> (Supplementary Information). Total renewable energy sources over time are similar but with solar instead of 40GW of offshore wind. The simulations consider the phase-out of conventional vehicles by 2030, in line with government policy, and a consistent move of aviation and freight towards biofuels, and electrified rail, as well as increased efficiency in buildings and use of heat pumps. These simulations provide outputs for the UK for 2020 to 2070 of CO<sub>2</sub> emissions per unit energy, total energy mix and output, labour costs, electricity costs, fuel costs, and road and rail transport costs that are inputs for calculating the costs of ERW CDR and secondary emissions during the grinding of rocks (Extended Data Fig. 2).

51. Palandri, J.L., Kharaka, Y.K. *A compilation of rate parameters of water-mineral interaction kinetics for application to geochemical modelling* (USGS Open File Report, 2004).
52. Lawrence, D.M. *et al.* The Community Land Model version 5: Description of new features, benchmarking, and impact of forcing uncertainty. *J. Adv. Model. Earth Sys.* **11**, 4245–4287 (2019).
53. Lawrence, D.M. *et al.* *Technical Description of version 5.0 of the Community Land Model (CLM)* (National Center for Atmospheric Research, Boulder, Co., pp. 1-337, 2020).
54. Wieder, W. R. *et al.* Beyond static benchmarking: Using experimental manipulations to evaluate land model assumptions. *Global Biogeochem. Cycles*, **33**, 1289–1309 (2019).
55. Lombardozzi, D. L. *et al.* Simulating agriculture in the Community Land Model Version 5. *J. Geophys. Res. Biogeosci.*, **125**, e2019JG005529 (2020).
56. Lawrence, D.M. *et al.* The Land Use Model Intercomparison Project (LUMIP) contribution to CMIP6: Rationale and experimental design. *Geosci. Mod. Dev.* **9**, 2973–2998 (2016).
57. Thomson, A. *et al.* *Quantifying the impact of future land use scenarios to 2050 and beyond*. (Rothamsted Research, Final Report for the Committee on Climate Change, IT/KB 0917, pp. 1-78, 2018).

58. DEFRA. *British Survey of Fertiliser Practice Fertiliser use on farm for the 2018 crop year* ([https://assets.publishing.service.gov.uk/government/uploads/system/uploads/attachment\\_data/file/806642/fertiliseruse-statsnotice2018-06jun19.pdf](https://assets.publishing.service.gov.uk/government/uploads/system/uploads/attachment_data/file/806642/fertiliseruse-statsnotice2018-06jun19.pdf)).
59. Fung, K.M., Val Martin, M. & Tai, A.P.K. Modeling the interinfluence of fertilizer-induced NH<sub>3</sub> emission, nitrogen deposition, and aerosol radiative effects using modified CESM2, *Biogeosciences Discuss.* [preprint], <https://doi.org/10.5194/bg-2021-63>, (2021).
60. IPCC. *IPCC Guidelines for National Greenhouse Gas Inventories Prepared by the National Greenhouse Gas Inventories Programme* (Eggleston H.S., Buendia L., Miwa K., Ngara T. and Tanabe K. eds, IGES, Japan, 2006).
61. IPCC. *Refinement to the 2006 IPCC Guidelines for National Greenhouse Gas Inventories* (Calvo Buendia, E., Tanabe, K., Kranjc, A., Baasansuren, J., Fukuda, M., Ngarize, S., Osako, A., Pyrozhenko, Y., Shermanau, P. and Federici, S. (eds), IPCC, Switzerland, 2019).
62. Hartmann, J. & Kempe, S. What is the maximum potential for CO<sub>2</sub> sequestration by “stimulated” weathering on the global scale? *Naturwissenschaften*, **95**, 1159-1164 (2008).
63. Taylor, L.L. *et al.* Increased carbon capture by a silicate-treated forested watershed affected by acid deposition. *Biogeosciences* **18**, 169-199 (2021).
64. Banwart, S.A., Berg, A. & Beerling, D.J. Process-based modelling of silicate mineral weathering responses to increasing atmospheric CO<sub>2</sub> and climate change. *Global Biogeochem. Cycles* **23**, GB4013 (2009).
65. Nelson, P.N. & Su, N. Soil pH buffering capacity: a descriptive function and its application to some acidic tropical soils. *Aust. J. Soil Sci.* **48**, 201-207 (2010).
66. Cerling, T. Carbon dioxide in the atmosphere: evidence from Cenozoic and Mesozoic paleosols. *Am. J. Sci.* **291**, 377–400 (1991).
67. Holland, J.E. *et al.* Yield responses of arable crops to liming – an evaluation of relationships between yields and soil pH from a long-term liming experiment. *Euro. J. Agron.* **105**, 176-188 (2019).
68. Holden, P.B., Edwards, N.R., Gerten, D. & Schaphoff, S. A model-based constraint on CO<sub>2</sub> fertilisation. *Biogeosci.* **10**, 339–355 (2013)
69. Holden, P.B. *et al.* Controls on the spatial distribution of oceanic  $\delta^{13}\text{C}$  DIC. *Biogeosci.* **10**, 1815–1833 (2013).
70. Foley, A.M. *et al.* Climate model emulation in an integrated assessment framework: a case study on mitigation policies in the electricity sector. *Earth Sys. Dyn.* **7**, 119-132 (2016).

71. Brown, T.J. *et al.* *Underground Mining of Aggregates Main Report* (ASRP Project No. 7 Assess the feasibility of the underground mining of aggregates, MA/1/S/7/01, British Geological Survey, Keyworth, pp. 1-322, 2010).
72. Van Vuuren, D.P., Bouwman, A.F. and Beusen, A.H.W. Phosphorus demand for the 1970-2100 period: A scenario analysis of resource depletion. *Global Environ Change* **20**, 428-439 (2010).
73. Alewell, C. *et al.* Global phosphorus shortage will be aggravated by soil erosion. *Nat Comms* **11**, 4546 (2020).
74. Gilbert, N. The disappearing nutrient. *Nature* **461**, 716-718 (2009).
75. Ciceri, D., Manning, D.A.C. & Allanore, A. Historical and technical developments of potassium resources. *Sci. Total Environ.* **502**, 590-601 (2015).
76. Agriculture and Horticulture Development Board, GB Fertilizer Prices (Agriculture and Horticulture Development Board, 2020). (<https://ahdb.org.uk/GB-fertiliser-prices>)
77. Wernet, G. *et al.* The ecoinvent database version 3 (part I): overview and methodology. *Int. J. Life Cycle Assess*, **21**, 1218-1230 (2016).
78. Hartmann, J. & Moosdorf, N. The new global lithological map database GLiM: A representation of rock properties at the Earth surface. *Geochem., Geophys., Geosys.* **13**, no. 12, doi Q1200410.1029/2012gc004370 (2012).
79. Ordnance Survey, *Strategy, road and rail vector data* (Ordnance Survey, GB. 2016).
80. Maguire, D.J. *ArcGIS: General Purpose GIS Software System*, in *Encyclopedia of GIS*, (S. Shekhar and H. Xiong, Eds, Springer US: Boston, MA. p. 25-31, 2008).
81. Wilkins, J., *Table TSGB0304 (ENV0104), Average heavy goods vehicle fuel consumption. Transport Statistics Great Britain 2017* (Department for Transport, London, 2017).
82. International Energy Agency. *The Future of Rail, Opportunities for energy and the environment* (International Energy Agency, 2019).
83. Delgado, O., Rodríguez, F. & Moncrieff, R. *Fuel Efficiency Technology in European Heavy-Duty Vehicles: Baseline and Potential for the 2020–2030 Time Frame*. (The International Council of Clean Transportation White paper, 2017).
84. SMMT, *Truck Specification for Best Operational Efficiency Guide* (Department for Transport, London, 2010).
85. MDS, *Analysis of road and rail costs between coal mines and power stations* (MDS Transmodal limited, 2012).
86. ORR, *Table 1350 - Rail freight market share, Freight rail usage and performance 2020-21 Quarter 3* (Office of Rail and Road. UK National Statistics, 2021).

87. Beeson, R., *The Rail Central Rail Freight Interchange, Appendix 21.2 Rail & Road Freight Emission Factors* (Turley, Editor. National Infrastructure Planning, 2018).
88. Liimatainen, H., van Vliet, O. & Aplyn, D. The potential of electric trucks – an international commodity-level analysis. *App. Energy* **236**, 804-814 (2019).
89. Mercure, J.F. *et al.* Macroeconomic impact of stranded fossil fuel assets. *Nat. Clim. Change* **8**, 588-593 (2018).
90. Cambridge Econometrics (2019) ‘E3ME Manual: Version 6.1’, available at [www.e3me.com](http://www.e3me.com)
91. Mercure, J-F. *et al.* Environmental impact assessment for climate change policy with the simulation-based integrated assessment model E3ME-FTT-GENIE’, *Energy Strat. Rev.*, **20**, 195–208 (2018).
92. HM Government. *The Energy White Paper. Powering our net zero future* (Open Government Licence, pp. 1-166, 2020).

## **Additional Information**

**Supplementary Information** is available for this paper at ....

**Reprints and permissions information** is available at [www.nature.com/reprints](http://www.nature.com/reprints).

**Correspondence and requests for materials** should be addressed to D.J.B. ([d.j.beerling@sheffield.ac.uk](mailto:d.j.beerling@sheffield.ac.uk))

**Data availability.** Soil pH data were obtained from <https://daac.ornl.gov/SOILS/guides/HWSD.html> and <http://www.ukso.org/>. The high-resolution monthly fields of soil temperature and precipitation data were obtained from [https://disc.gsfc.nasa.gov/datasets/FLDAS\\_NOAH01\\_C\\_GL\\_M\\_001/summary](https://disc.gsfc.nasa.gov/datasets/FLDAS_NOAH01_C_GL_M_001/summary). Additional environmental and climate drivers were acquired through simulations of the Community Land Model (CLM5) version 5.0 available at <https://github.com/ESCOMP/ctsm>. The UK crop cover map from <https://www.ceh.ac.uk/ukceh-land-cover-maps>, annual time series of crop yields from <https://www.fao.org/faostat/en/#data> and UK fertilizer usage data from <https://www.gov.uk/government/collections/fertiliser-usage>. UK national border data from [https://thematicmapping.org/downloads/world\\_borders.php](https://thematicmapping.org/downloads/world_borders.php). The GLiM v1.0 dataset used to identify rock sources is available at <https://www.geo.uni->

[hamburg.de/en/geologie/forschung/aquatische-geochemie/glim.html](http://hamburg.de/en/geologie/forschung/aquatische-geochemie/glim.html). Dataset with 5 minute resolution on global crop production and yield area to identify cropland is available at <http://www.earthstat.org/harvested-area-yield-175-crops/>. Datasets on roads and rails vector data used for countries transport network analysis are available at <http://www.diva-gis.org/gdata>. Datasets on LCA impact factors used for K and P fertilizers are available within Ecoinvent 3.6 at <https://ecoinvent.org/>.

**Code availability.** The weathering model was developed in MATLAB v.R2019a, data processing in both MATLAB v.R2019a and Python v.3.7. MATLAB and Python codes developed for this study belong to the Leverhulme Centre for Climate Change Mitigation. The authors will make these codes and the modified codes in CLM5 developed in this study available upon reasonable request.

**Source data.** Source datasets for Figures and Extended Data Figures are uploaded.